

# Synthesis, characterization and photoluminescence properties of graphene oxide functionalized with azo molecules

R DEVI<sup>a</sup>, G PRABHAVATHI<sup>c</sup>, R YAMUNA<sup>a,\*</sup>, S RAMAKRISHNAN<sup>b</sup>  
and NIKHIL K KOTHURKAR<sup>b</sup>

<sup>a</sup>Department of Sciences, <sup>b</sup>Department of Chemical Engineering and Material Science, Chemistry and Materials Research Laboratory, Amrita Vishwa Vidhyapeetham, Coimbatore 641 112, India

<sup>c</sup>Research and Development Centre, Bharathiyar University, Coimbatore 641 112, India  
e-mail: r\_yamuna@cb.amrita.edu

MS received 1 May 2013; revised 19 September 2013; accepted 19 September 2013

**Abstract.** Two different azo molecules functionalized graphene oxide (GO) through an ester linkage have been synthesized for the first time. Chemical structure of the azo-GO hybrids was confirmed by Fourier transform infrared spectroscopy and UV-visible spectroscopy. The GO functionalized with 5-((4-methoxyphenyl)azo)-salicylaldehyde was further characterized by scanning electron microscopy (SEM), transmission electron microscopy (TEM), and atomic force microscopy (AFM). The SEM studies demonstrated that the morphology of the azo-GO hybrid was found to be similar to the GO sheets but slightly more wrinkled. Further, TEM image of azo-GO indicates some dark spots on the GO sheets due to azo functionalization. AFM results also reveal that the azo functionalization increases the thickness of GO sheet to 4–5 nm from 1.2–1.8 nm. Both the azo-hybrids show absorption band around 379 nm due to the  $\pi$ - $\pi^*$  transition of the *trans* azo units. Photoluminescence spectra of azo-GO hybrids show a strong quenching compared with azo molecules due to the photoinduced electron or energy transfer from the azo chromophore to the GO sheets. It also reveals strong electronic interaction between azo and GO sheets.

**Keywords.** Azo benzene functionalized graphene oxide; photo switching; azo/GO hybrid; covalent functionalization; photochromic molecules.

## 1. Introduction

Photochromic compounds, which can easily undergo large conformational changes when exposed to light of appropriate wavelength, are fascinating as molecular switching devices.<sup>1</sup> Azobenzenes are one among the photo switching molecules that fulfill this condition.<sup>2</sup> Due to its clean photochemistry, and substantial change in material properties during light irradiation, these molecules have been employed in a variety of applications such as optical data storage,<sup>3</sup> photo switching technologies,<sup>4</sup> liquid crystals,<sup>5</sup> chemo sensors<sup>6</sup> and as sensitizer in dye sensitized solar cells (DSSC).<sup>7</sup> They are readily synthesized and easily characterized by <sup>1</sup>H NMR, UV visible spectroscopy (UV-Vis) and Fourier transform infrared (FT-IR) spectroscopy. When irradiated with an appropriate wavelength of light,<sup>8</sup> azo benzene molecules undergo *cis-trans* isomerization which enables them to act as photo switchable core because of their thermal stability, detectability, high sensitivity

and reversibility. These photochromic molecules undergo *cis-trans* isomerization with high quantum efficiencies. Materials containing even small amount of azo molecules have been shown to effect a substantial change in optical properties and morphologies.<sup>9,10</sup>

Graphene<sup>11</sup> as a unique 2D nanocarbon material, has attracted significant interest owing to its distinctive structure, outstanding electronic, thermal and mechanical properties.<sup>12–14</sup> Graphene is one of the best candidates for numerous applications such as nanoelectronics, gas sensors, organic photovoltaics, field-effect transistors and other nanocomposites.<sup>15–19</sup> Though there are numerous reports on the many exceptional properties, and applications of both single and multi-walled carbon nanotubes (CNT)<sup>20</sup> and fullerenes,<sup>21</sup> such intensive research is expected for graphene as a building block for new nanomaterials. However, the solubility and processability of this graphene in variety of solvents are the main issues for many diverse applications of graphene-based materials. This solubility problem can be minimized by using graphene oxide (GO),<sup>10,22–27</sup> which is the oxygenated form of monolayer graphene platelets. This allows chemical functionalization of GO

\*For correspondence

with variety of organic molecules, which will generate new materials with more interesting properties for further applications.<sup>28,29</sup> One major advantage of using GO is its bulk synthesis from natural graphite by chemical oxidation and subsequent exfoliation. The hydrophilic surface functional groups such as epoxide, hydroxyl, and carboxyl groups of GO makes it more water soluble and enables further chemical modification of graphene.<sup>23,30</sup>

CNT and GO have been functionalized with chromophores in order to facilitate photo absorptivity in case of photochemical devices.<sup>8,17</sup> Solar thermal fuel, composed of azobenzene functionalized with carbon nanotubes has been reported in the literature.<sup>31</sup> It has been reported that the number of photoactive molecules per unit volume (i.e., photo isomer concentration) is significantly increased with respect to a solution of free photo molecules, leading to an increased volumetric energy density of 5–7 orders of magnitude due to the highly ordered array of adsorbed photo molecules with CNT substrate.<sup>31</sup> Hybrids of azo/CNT<sup>8</sup> and azo/GO<sup>32</sup> through noncovalent interaction and an amide linkage, respectively, were also studied for photo switching properties. Graphene azo poly electrolyte multilayer fabricated by electrostatic layer by layer also has been investigated for electrochemical capacitor electrode.<sup>33</sup> Recently, there is a report on the preparation of graphene grafted with azo polymer and its photo responsive properties.<sup>34</sup> In this study, we have functionalized GO with two types of azo chromophoric compounds, 5-((4-methoxyphenyl)azo)-salicylaldehyde (azoGO-I) and 5-((4-ethoxyphenyl)azo)-salicylaldehyde (azoGO-II) through an ester linkage. We have chosen the azo molecules in such a way that one end of this organic molecule has electron donating group (methoxy, ethoxy) and other end contains electron withdrawing group (salicylaldehyde). We anticipate that this will act as push-and-pull-like molecular system which in turn will increase the photoinduced electron or energy transfer from the azo chromophore to the GO sheets. The synthesized azo-GO hybrids were characterized by FTIR and UV-Vis. The azo-GO hybrid (I) has been further characterized by transmission electron microscopy (TEM), atomic force microscopy (AFM), and scanning electron microscopy (SEM). The photophysical properties of azo-GO hybrids I and II are also reported.

## 2. Experimental

### 2.1 Materials

Thionyl chloride (SOCl<sub>2</sub>), 4-methoxyaniline (Aldrich), 4-ethoxyaniline (Aldrich), and salicylaldehyde (Aldrich)

are used as received. Solvents such as N, N-dimethyl formamide (DMF), di-methyl sulphoxide (DMSO), ethyl acetate, chloroform, dry tetrahydrofuran (THF), and ethanol were purified and distilled using standard procedure.

### 2.2 Characterization and instrumentation

FT-IR spectra were recorded in Thermo Nicolet, iS10 FT-IR spectrometer using KBr disk method. Absorption spectra were carried out using Shimadzu, UV 1800 spectrophotometer. <sup>1</sup>H nuclear magnetic resonance (NMR) spectra were measured in JEOL 300 MHz multinuclear spectrometers in CDCl<sub>3</sub>. Chemical shift was expressed in parts per million (ppm) relative to TMS. SEM images were recorded using F E I Quanta FEG 200-High Resolution Scanning Electron Microscope (HRSEM). Elemental analysis was carried out in PerkinElmer series II CHNS/O elemental analyser 2400. Photo luminescence (PL) spectra were recorded using Shimadzu RF-5301 PC spectro fluoro photometer. Powder X-ray diffractograms were performed at room temperature on a Bruker D8 Focus X-ray diffractometer, using Ni-filtered Cu K $\alpha$  radiation ( $\lambda = 1.541 \text{ \AA}$ ) with a scintillator detector (40 kV, 40 mA). The step time was 1 s at 0.04°/step in a  $2\theta$  range of 5–90°. High Resolution Transmission Electron Microscope (HRTEM) image was obtained by using the JEOL JEM 2100 transmission electron microscope. AFM carried out by using NTEGRA Prima-NT-MDT.

### 2.3 Synthesis of 5-((4-methoxyphenyl)azo)-salicylaldehyde (Ia)

4-Methoxyaniline (1 g, 8.12 mmol) was added to 3.60 ml of 6.00 M hydrochloric acid at 0–5°C. Sodium nitrite (0.57 g, 8.24 mmol in 3.60 ml of H<sub>2</sub>O) was added dropwise to the reaction mixture for 30 min under constant mechanical stirring. A solution of salicylaldehyde (0.99 g, 8.12 mmol) in 3.60 ml of 10% NaOH was added slowly to the diazonium salt over the period of 1 h at 0–5°C. Dilute acetic acid was added to the formed brownish orange precipitate. The precipitate was washed with NaHCO<sub>3</sub> and dried with anhydrous Na<sub>2</sub>SO<sub>4</sub>. Resulting orange colour solution was dried under reduced pressure and purified on silica gel (100–200 mesh) column using ethyl acetate, chloroform mixture (1:9). Yield: 1.56 g, (75%), *R<sub>f</sub>* value is 0.86. FT-IR (in cm<sup>-1</sup>): 1654 (C=O), 1454 (N=N), 2926, 2847 (Aliphatic C–H Str.), 3180 (Aromatic C–H str.), 3426 (–OH str.). NMR data in CDCl<sub>3</sub>,  $\delta = 10.06$  (s, aldehyde H), 3.94 (s, –OCH<sub>3</sub>), 8.18 (d, aromatic 2H), 7.94 (d, aromatic 2H), 7.16 (d, aromatic 1H), 7.07 (d, aromatic 2H) ppm (for NMR spectra, see supporting information figure S1).

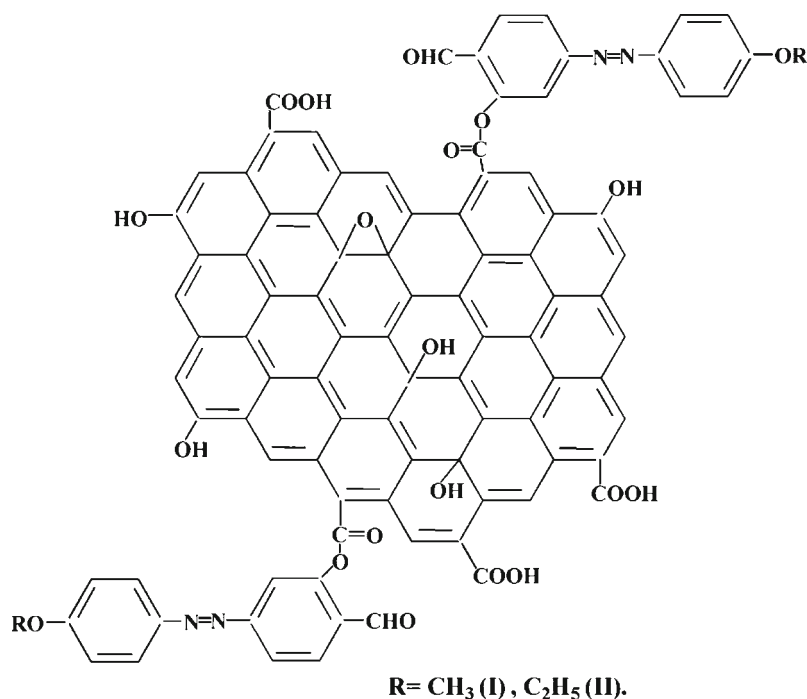


**Figure 1.** Structure of azo-GO hybrids (**I** and **II**).

$C_{14}H_{12}N_2O_3$  (256.26): calcd. C 65.62, H 4.72, N 10.93; found C 65.73, H 4.65, N 10.62. The same procedure was followed for synthesizing (**2a**) by using 4-ethoxyaniline instead of 4-methoxyaniline.

#### 2.4 5-((4-Ethoxyphenyl) azo)-salicylaldehyde (**2a**)

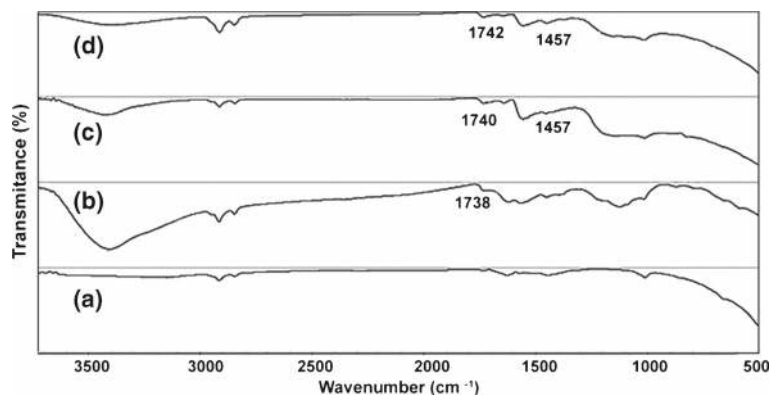
Yield: 1.44 g, (73%),  $R_f$  value is 0.93. FT-IR (in  $cm^{-1}$ ): 1661 (C=O), 1472 (N=N), 2976, 2926 (Aliphatic C-H Str.), 3068 (Aromatic C-H str.), 3414 (-OH str.). NMR data in  $CDCl_3$ , 25°C, TMS:  $\delta$  = 10.05 (s, aldehyde H), 1.51 (t, alkyl 3H), 4.16 (q, -OCH<sub>2</sub>), 8.12 (d, aromatic 2H), 7.93 (d, aromatic 2H), 7.15 (d, aromatic 1H), 7.05 (d, aromatic 2H) ppm.  $C_{15}H_{14}N_2O_3$  (270.29): calcd. C 66.66, H 5.22, N 10.36; found C 65.73, H 5.39, N 10.21.

#### 2.5 Synthesis of acyl chloride functionalized graphene oxide (GOCl)

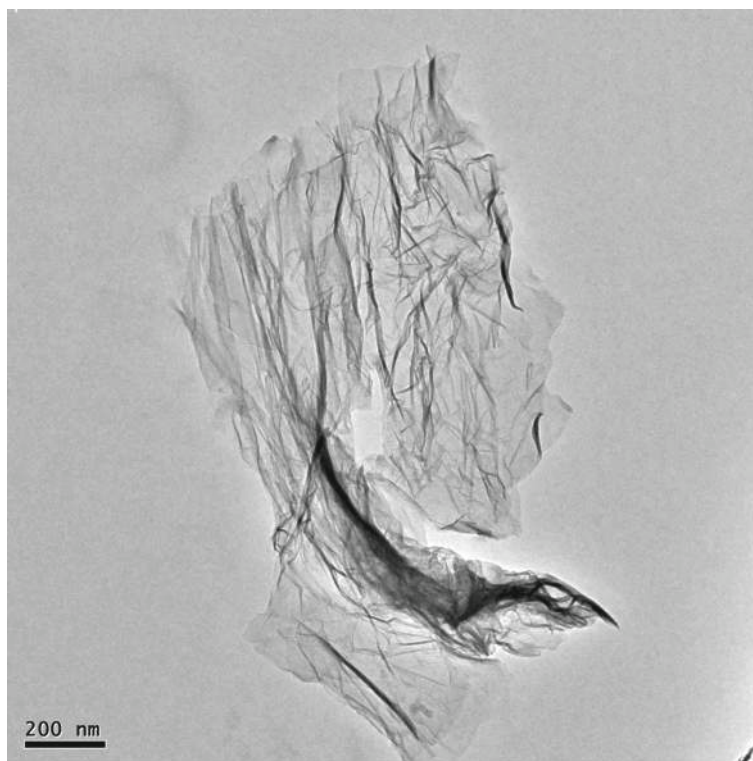
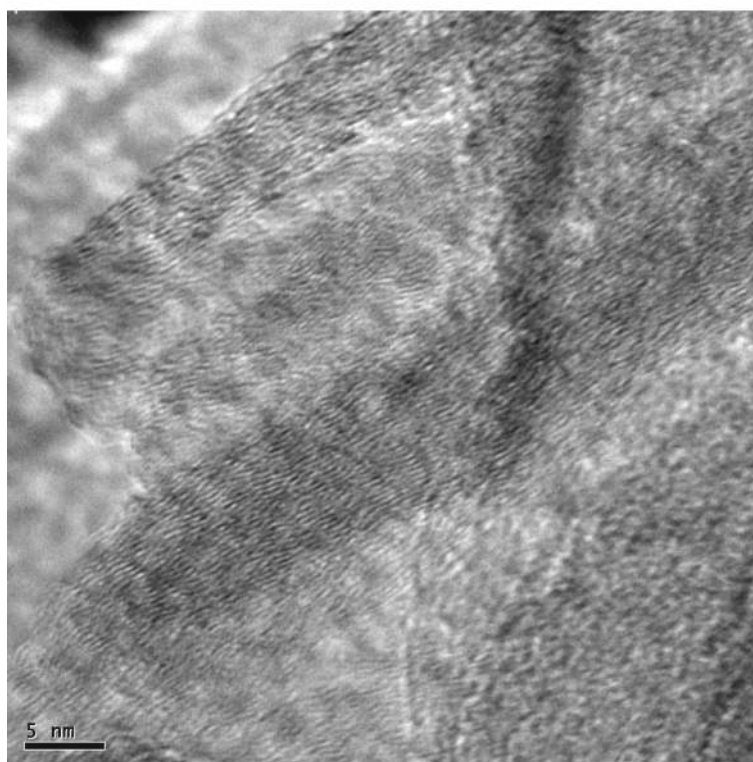
GO (30 Mg) was refluxed with  $SOCl_2$  (20 ml) in the presence of DMF (0.5 mL) at 65–70°C for 24 h under argon atmosphere to form acyl chloride functionalized GO (GOCl). Excess solvent and  $SOCl_2$  were removed by distillation.

#### 2.6 Synthesis of 5-((4-methoxyphenyl)azo)-salicylaldehyde functionalized GO (**I**)

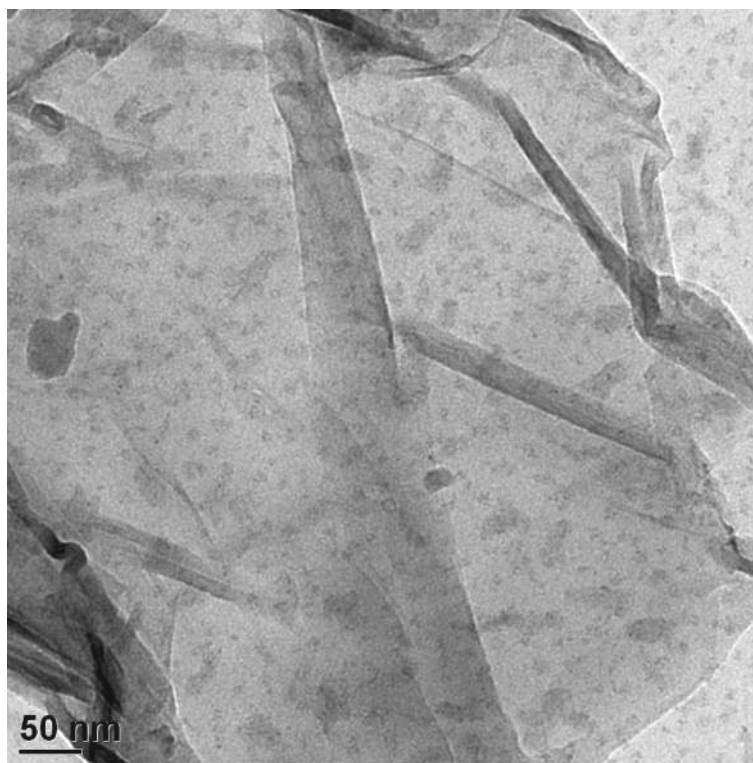
GOCl (100 Mg) and 0.58 mmol of 5-((4-methoxyphenyl)azo)-salicylaldehyde (**1a**) were dissolved in DMSO (20 ml) and refluxed at 50°C for 65 h under  $N_2$  atm. After completion of the reaction, the product was cooled



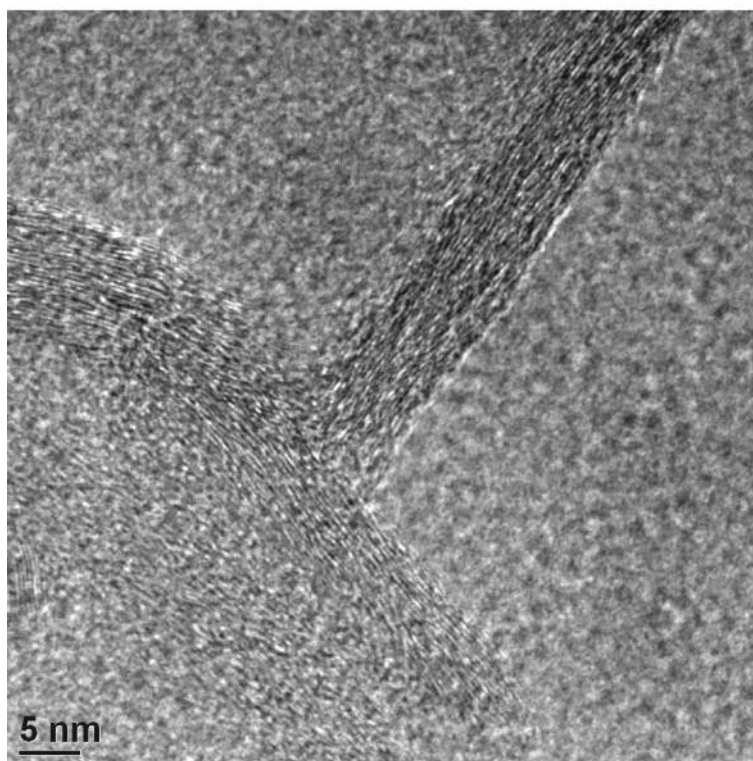
**Figure 2.** FT-IR spectra of (a) pure graphite, (b) graphene oxide, (c) methoxy azo-GO hybrid (**I**) and (d) ethoxy azo-GO hybrid (**II**).

**(a)****(b)****Figure 3.** a and b. TEM images of the GO.





(a)



(b)

**Figure 4.** a and b. TEM images of the methoxy azo-GO hybrid (I).

to room temperature. The precipitate was ultra centrifuged and excess azo impurity was removed by washing with ethanol until the solution became colourless.

### 2.7 Synthesis of 5-((4-ethoxyphenyl)azo)-salicylaldehyde functionalized GO (II)

This azoGO-II hybrid was synthesized by following the above procedure with 5-((4-ethoxyphenyl)azo)-salicylaldehyde (**2a**) instead of 5-((4-methoxyphenyl)azo)-salicylaldehyde.

## 3. Results and discussion

### 3.1 Synthesis and structure of the Azo-GO I and II hybrids

Water soluble GO was prepared from graphite flakes ( $<20\ \mu\text{m}$ ; Sigma Aldrich) using Hummers method.<sup>30</sup> Distinctive powder X-ray diffractograms features of graphite and the synthesized GO are given in the supporting information (figure S2). For the graphite sample, the characteristic peak of hexagonal graphite corresponding to a d-spacing of 0.34 nm was found at  $26.66^\circ$ . Upon conversion of the graphite into GO, the peak position shifted to a lower diffraction angle of  $10.52^\circ$  with an increase in the interlayer spacing of 0.84 nm. Disappearance of graphite diffraction peak at  $26.66^\circ$  confirms the oxidation of graphite to GO.<sup>35</sup> This increase in d-spacing is due to the intercalation of various oxygen species mostly ether ring oxygen and hydroxyl functional groups in between the graphene layers.

The soluble 5-((4-methoxyphenyl)azo)salicylaldehyde-GO (**I**) and 5-((4-ethoxyphenyl)azo)salicylaldehyde-GO hybrids (**II**) were synthesized by suitable modification of literature procedure.<sup>32</sup> 5-((4-Methoxyphenyl)azo)-salicylaldehyde (**1a**) and 5-((4-ethoxyphenyl)azo)-salicylaldehyde (**2a**) were covalently linked to GO molecules through an ester bond by refluxing appropriate azo compound with GO in DMSO at  $50^\circ\text{C}$  for 65 h under  $\text{N}_2$  atm. The chemical structure of the compound is shown in figure 1. The azo/GO hybrid structures have been confirmed by FT-IR spectra in the range of  $500\text{--}4000\ \text{cm}^{-1}$  as shown in figure 2. GO contains various functional groups including ether, epoxide, carboxylic acid, phenolate and aldehyde groups. The characteristic absorption peak assigned to carbonyl ( $\text{--C=O}$ ) stretching mode of GO, azo-GO **I** and **II** is clearly visible at  $1738$ ,  $1740$  and  $1742\ \text{cm}^{-1}$ , respectively as shown in figure 2b–d.<sup>32</sup> After functionalization, a new striking peak at  $1457\ \text{cm}^{-1}$  in figure 2c and d of hybrids (**I**) and

(**II**) confirms the stretching mode of ( $\text{--N=N--}$ ) bond.<sup>36</sup> The three peaks in the range of  $1020\text{--}1162\ \text{cm}^{-1}$  (figure 2c and d) reveal the presence of  $\text{--C--O--}$  stretching mode of an ester linkage.<sup>37</sup>

Morphologies of GO and azo functionalized GO (**I**) were investigated by SEM. SEM images of GO and azo-GO (**I**) sheet morphology over a few micron length scales are given in supporting information (figures S3 and S4). Figure S4 reveals that the graphene sheets in the azo-GO hybrid somewhat are more wrinkled than GO sheet (see figure S3) due to azo functionalization.

Thickness and morphology of the GO and azo-GO (**I**) were further probed using AFM. AFM images of GO deposited on freshly cleaved mica surface and its height profile line are given in supporting information (see figure S5 (a) and (b)). From the figure, thickness of the GO layer is found to be  $\approx 1.2\text{--}1.8\ \text{nm}$  (one to two layers), which is due to conversion of graphene to GO.<sup>38,39</sup> The AFM images of azo-GO hybrid (**I**) and its height profile line are given in supporting information (see figure S6 (a) and (b)). This figure indicates that the thickness of azo functionalized GO sheet is  $\approx 4\text{--}5\ \text{nm}$  (four to six

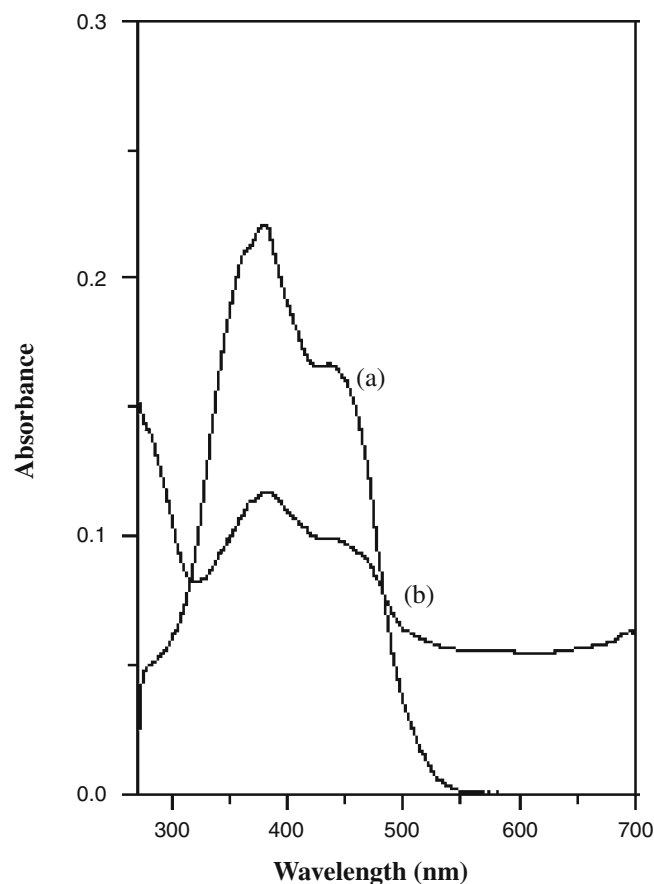


**Figure 5.** Absorption spectra of (a) methoxy azo (**1a**) ( $1.4 \times 10^{-5}\ \text{M}$ ) and (b) methoxy azo-GO hybrid (**I**) ( $1.5\ \text{mg}/100\ \text{ml}\ \text{DMF}$ ).

layers). Thickness of the GO sheet increases after functionalization with methoxy azo due to the stacking of the layers, which is similar to other reported results.<sup>40</sup>

TEM images of GO and azo-GO (**I**) are shown in figures 3 and 4. Figure 4a depicts the TEM images of azo-GO where some dark spots can be observed on the GO sheets due to azo functionalization. Figures 3b and 4b show stacked GO and azo-GO sheets with an interlayer spacing of  $\approx 0.60$  and 0.65 nm for GO and azo-GO, respectively. Compared to the pure graphene interlayer distance of 0.34 nm, an interspacing of 0.60 nm indicates fully oxidized graphene.<sup>41</sup> Azo functionalized GO has slightly higher interlayer spacing 0.65 nm compared to GO.

### 3.2 Spectroscopy measurements

Figures 5 and 6 show UV-vis absorption spectra of 5-((4-methoxyphenyl) azo)-salicylaldehyde (**1a**), 5-((4-ethoxyphenyl) azo)-salicylaldehyde (**2a**) and azo-GO hybrids **I** and **II** in DMF solvent. UV-vis spectrum of azo salicylaldehyde (**1a**) and (**2a**) shows an intense band around 379 nm in DMF solvent which is due to the  $\pi-\pi^*$  transition of the *trans* azo units.<sup>42</sup> We also confirmed this  $\pi-\pi^*$  transition peak by recording the spectra for (**1a**) and (**2a**) in nonpolar DCM solvent; we observed that this peak shifted to shorter wavelength (around 354 nm). The azo-GO hybrids **I**, **II** and

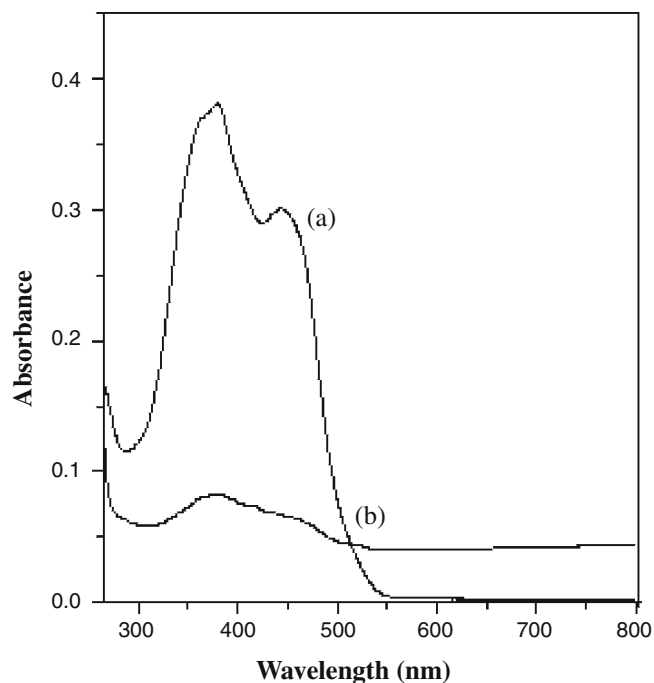


**Figure 6.** Absorption spectra of (a) ethoxy azo (**2a**) ( $3.3 \times 10^{-5}$  M) and (b) ethoxy azo-GO hybrid (**II**) (1 mg/100 ml DMF).

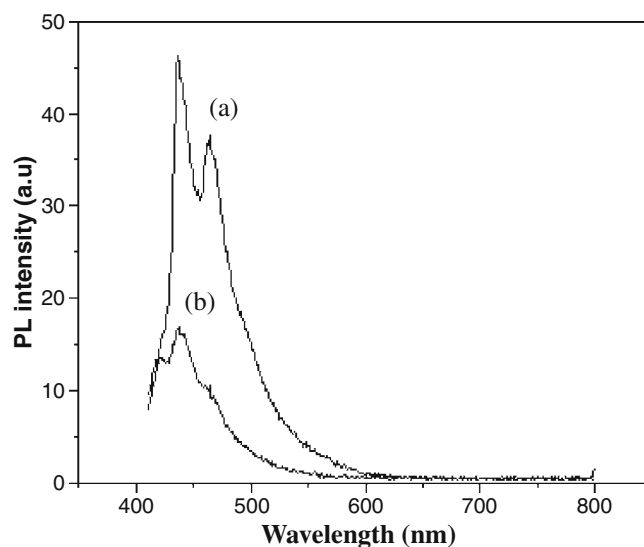


**Figure 7.** PL spectra of (a) methoxy azo (**1a**) ( $1.4 \times 10^{-5}$  M) and (b) methoxy azo/GO (**I**) (3 mg/100 ml DMF) ( $\lambda_{\text{ex}} = 400$  nm) with the same absorbance value at the  $\pi-\pi^*$  transition (Abs = 0.24).

the pristine azo molecules also exhibit a peak around 450 nm which is absent in the reported azo-GO hybrid and 2-aminoazotoluene.<sup>32</sup> The  $\pi-\pi^*$  transition peak of azo-GO hybrids **I**, **II** and the neat azo molecules shows a blue shift of about 22 nm compared to that of reported azo-GO hybrid and the pristine azo chromophore.<sup>32</sup> In figures 5b and 6b, intensity of the peaks are reduced considerably due to covalent functionalization of GO with azo molecules through an ester linkage. This is in agreement with the reported azo-GO hybrid where a similar suppression was observed between the

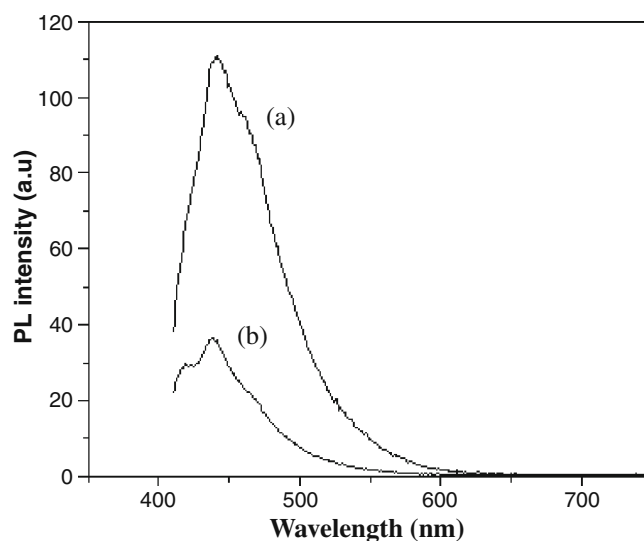


**Figure 8.** PL spectra of (a) ethoxy azo (**2a**) ( $1.3 \times 10^{-5}$  M) and (b) ethoxy azo/GO (**II**) (3 mg/100 ml DMF) ( $\lambda_{\text{ex}} = 400$  nm) with the same absorbance value at the  $\pi-\pi^*$  transition (Abs = 0.24).



azo-GO compared to pristine azo.<sup>32</sup> This indicates the interaction between the electronic energy level of azo molecules and GO in the azo-GO hybrids.<sup>29</sup>

Photoluminescence spectra of azo compounds (**1a**), (**2a**) and azo-GO hybrids (**I**) and (**II**) in DMF (excitation wavelength is 400 nm) are shown in figures 7 and 8. Emission spectra of these compounds show two peaks which is similar to the reported azo and azo-GO hybrids.<sup>32</sup> Whereas in the present study, a blue shift was observed in the azo-GO hybrids (**I**) and (**II**) compared to pure azo molecules. Emission spectra of these compounds also shows a blue shift compared to the reported azo-GO hybrid and its pristine azo molecule.<sup>32</sup> Figures 7b and 8b show strong quenching compared with pure azo molecules due to the photoinduced electron or energy transfer from the azo chromophore to the GO sheets. This is in agreement with the reported azo-GO hybrid where a similar suppression was observed between the azo-GO compared to pure azo (excitation wavelength is 480 nm).<sup>32</sup> Photoluminescence measurements demonstrate strong electronic interaction between azo group and GO sheets.

#### 4. Conclusion

Thus, we have successfully synthesized two different azo functionalized graphene oxides through an ester linkage for the first time. Chemical structure of the azo-GO hybrids were testified by the FT-IR spectra. A new peak at  $1457\text{ cm}^{-1}$  in IR spectra of hybrids **I** and **II** confirms the stretching mode of ( $-\text{N}=\text{N}-$ ) bond. SEM morphology studies demonstrated that chemical modification has a strong impact on the structure of GO sheets, forming tiny wrinkles on the graphene film. TEM image of azo-GO indicates some dark spots on the GO sheets due to azo functionalization. AFM results also reveal that the azo functionalization increases the thickness of GO sheet to 4–5 nm from 1.2–1.8 nm. Both the azo-GO hybrids show the absorption band around 379 nm due to the  $\pi-\pi^*$  transition of the *trans* azo units. Photoluminescence spectra of azo-GO hybrids show strong quenching compared with azo molecules due to the photoinduced electron or energy transfer from the azo chromophore to the GO sheets. It also reveals strong electronic interaction between azo and GO sheets. This result indicates that the azo-GO hybrids can become potential candidates for optoelectronic devices.

#### Supplementary information

Figures S1–S6 as supplementary information can be seen in [www.ias.ac.in/chemsci](http://www.ias.ac.in/chemsci) website.

#### Acknowledgements

The authors RY and RD thank the Council of Scientific and Industrial Research (CSIR), (Project No: 01(2256)/08/EMR-II), New Delhi, India for funding and Amrita Vishwa Vidyapeetham for infrastructure.

#### References

- Willner I 1997 *ACC. Chem. Res.* **30** 347
- Renner C and Moroder L 2006 *Chem. Bio. Chem.* **7** 868
- Kanis D R, Ratner M A and Marks T J 1994 *Chem. Rev.* **94** 195
- Feringa B L, van Delden R A, Koumura N and Geertsema E M 2000 *Chem. Rev.* **100** 1789
- Ikeda T and Tsutsumi O 1995 *Science* **268** 1873
- Bhardwaj V K, Singh N, Hundal M S and Hundal G 2006 *Tetrahedron* **62** 7878
- Mikroyannidis J A, Tsagkournos D V, Balraju P and Sharma G D 2011 *J. Power Sources* **196** 4152
- Simmons J M, In I, Campbell V E, Mark T J, Leonard F, Gopalan P and Eriksson M A 2007 *Phys. Rev. Lett.* **98** 086802
- Yager K G and Barrett C J 2001 *Curr. Opin. Solid State Mater. Sci.* **5** 487
- Yager K G and Barrett C J 2006 *J. Photochem. Photobiol.* **A182** 250
- Nikolaev A V, Bibikov A V, Avdeenkov A V, Bodrenko I V and Tkalya E V 2009 *Phys. Rev.* **B79** 045418
- Tsoukleri G, Parthenios J, Papagelis K, Jalil R, Ferrari A C, Geim A K, Novoselov K S and Galiotis C 2009 *Small* **5** 2397
- Rafiee M A, Rafiee J, Srivastava I, Wang Z, Song H, Yu Z-Z and Koratkar N 2010 *Small* **6** 179
- Zhou X, Wu T, Ding K, Hu B, Hou M and Han B 2010 *Chem. Commun.* **46** 386
- Li X, Wang X, Zhang L, Lee S and Dai H 2008 *Science* **319** 1229
- Geim A K and Novoselov K S 2007 *Nat. Mater.* **6** 183
- Liu Z, Liu Q, Huang Y, Ma Y, Yin S, Zhang X, Sun W and Chen Y 2008 *Adv. Mater.* **20** 3924
- Gilje S, Han S, Wang M, Wang K L and Kaner R B 2007 *Nano Lett.* **7** 3394
- Hao R, Qian W, Zhang L and Hou Y 2008 *Chem. Commun.* **0** 6576
- Ajayan P M 1999 *Chem. Rev.* **99** 1787
- Martin N, Sanchez L, Illescas B and Perez I 1998 *Chem. Rev.* **98** 2527
- Niyogi S, Bekyarova E, Itkis M E, McWilliams J L, Hamon M A and Haddon R C 2006 *J. Am. Chem. Soc.* **128** 7720
- Stankovich S, Piner R D, Nguyen S T and Ruoff R S 2006 *Carbon* **44** 3342
- Si Y and Samulski E T 2008 *Nano Lett.* **8** 1679
- Qian W, Cui X, Hao R, Hou Y and Zhang Z 2011 *ACS Appl. Mater. Interfaces* **3** 2259
- Qian W, Hao R, Hou Y, Tian Y, Shen C, Gao H and Liang X 2009 *Nano Res.* **2** 706



27. Cui X, Zhang C, Hao R and Hou Y 2011 *Nanoscale* **3** 2118
28. Gomez-Navarro C, Burghard M and Kern K 2008 *Nano Lett.* **8** 2045
29. Yamuna R, Ramakrishnan S, Dhara K, Devi R, Kothurkar N, Kirubha E and Palanisamy P K 2013 *J. Nanopart. Res.* **15** 1
30. Hummers W S and Offeman R E 1958 *J. Am. Chem. Soc.* **80** 1339
31. Kolpak A M and Grossman J C 2011 *Nano Lett.* **11** 3156
32. Zhang X, Feng Y, Lv P, Shen Y and Feng W 2010 *Langmuir* **26** 18508
33. Wang D and Wang X 2010 *Langmuir* **27** 2007
34. Wang D, Ye G, Wang X and Wang X 2011 *Adv. Mater.* **23** 1122
35. Yeh T-F, Syu J-M, Cheng C, Chang T-H and Teng H 2010 *Adv. Funct. Mater.* **20** 2255
36. Albayrak C, Gumrukcuoglu I E, Odabasoglu M, Iskeleli N O and Agar E 2009 *J. Mol. Struct.* **932** 43
37. Deng Y, Li Y, Dai J, Lang M and Huang X 2011 *J. Polym. Sci. Part A: Polym. Chem.* **49** 4747
38. Akhavan O 2010 *Carbon* **48** 509
39. Subrahmanyam K S, Vivekchand S R C, Govindaraj A and Rao C N R 2008 *J. Mater. Chem.* **18** 1517
40. Geng J and Jung H-T 2010 *J. Phys. Chem. C* **114** 8227
41. Lahaye R J W E, Jeong H K, Park C Y and Lee Y H 2009 *Phys. Rev.* **B79** 125435
42. Gokulnath S, Prabhuraja V, Sankar J and Chandrashekar T K 2007 *Eur. J. Org. Chem.* **2007** 191